

PoseWatch: A Transformer-based Architecture for Human-centric Video Anomaly Detection Using Spatio-temporal Pose Tokenization

Ghazal Alinezhad Noghre^{1*}, Armin Danesh Pazho¹ and Hamed Tabkhi¹

¹Department of Electrical and Computer Engineering, University of North Carolina at Charlotte, USA.

*Corresponding author(s). E-mail(s): galinezh@charlotte.edu;
Contributing authors: adaneshp@charlotte.edu; htabkhiv@charlotte.edu;

Abstract

Video Anomaly Detection (VAD) presents a significant challenge in computer vision, particularly due to the unpredictable and infrequent nature of anomalous events, coupled with the diverse and dynamic environments in which they occur. Human-centric VAD, a specialized area within this domain, faces additional complexities, including variations in human behavior, potential biases in data, and substantial privacy concerns related to human subjects. These issues complicate the development of models that are both robust and generalizable. To address these challenges, recent advancements have focused on pose-based VAD, which leverages human pose as a high-level feature to mitigate privacy concerns, reduce appearance biases, and minimize background interference. In this paper, we introduce PoseWatch, a novel transformer-based architecture designed specifically for human-centric pose-based VAD. PoseWatch features an innovative Spatio-Temporal Pose and Relative Pose (ST-PRP) tokenization method that enhances the representation of human motion over time, which is also beneficial for broader human behavior analysis tasks. The architecture's core, a Unified Encoder Twin Decoders (UETD) transformer, significantly improves the detection of anomalous behaviors in video data. Extensive evaluations across multiple benchmark datasets demonstrate that PoseWatch consistently outperforms existing methods, establishing a new state-of-the-art in pose-based VAD. This work not only demonstrates the efficacy of PoseWatch but also highlights the potential of integrating Natural Language Processing techniques with computer vision to advance human behavior analysis.

Keywords: Video Anomaly Detection, Human Centric, Human Pose, Privacy-Preserving, Human Behavior Analysis, Transformers

Statements and Declarations

This research is funded and supported by the United States National Science Foundation (NSF) under Award Numbers 1831795 and 2329816.

All datasets used in this manuscript are publicly available.

1 Introduction

Video Anomaly Detection (VAD) is a rapidly growing area within Computer Vision that focuses on automatically identifying unusual events or behaviors in video sequences (Ren et al., 2021; Patrikar and Parate, 2022; Abbas and Al-Ani,

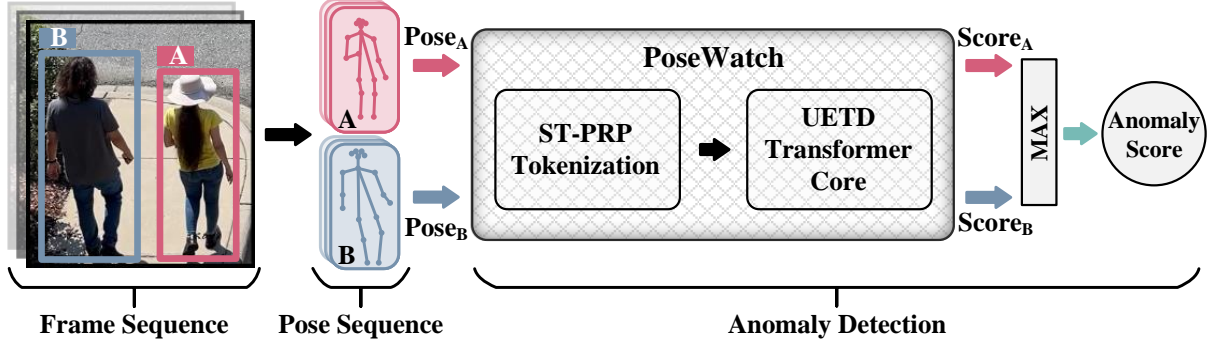


Fig. 1 A conceptual overview of PoseWatch. PoseWatch assigns higher scores to anomalous pose sequences. The final frame score is the maximum score of all individuals in the scene.

2022; Ramachandra et al., 2020). This technology has a wide array of practical applications, including smart surveillance (Pazho et al., 2023; Patrikar and Parate, 2022), traffic monitoring (Zhao et al., 2023; Yu and Huang, 2022; Pazho et al., 2024), and healthcare (Nanda et al., 2022). A notable subset of VAD is human-centric anomaly detection, which specifically targets the recognition of atypical human behaviors.

The complexity of this task stems from its open-set nature, where an immense variety of normal and abnormal human behaviors can occur in real-world situations. For example, anomalies could include someone falling, engaging in a physical altercation, or causing unusual congestion in public spaces (Zhu et al., 2022). The core challenge is the unpredictability and diversity of these events. Traditional supervised training methods, which depend on datasets that may not cover the full spectrum of possible anomalies, struggle with generalizability (Alinezhad Noghre et al., 2023). This is because anomalies, by definition, are often unknown and unexpected.

To overcome these challenges, the field is increasingly embracing self-supervised learning approaches. These innovative methods enhance the performance of anomaly detection models by learning from normal data without needing explicit labels or fine-grained categories for anomalies (Markovitz et al., 2020; Hirschorn and Avidan, 2023; Morais et al., 2019). In essence, self-supervised models develop an understanding of normal human behavior patterns. Consequently, any deviation from these learned patterns is identified as an anomalous event. In this paper,

we adopt the self-supervised learning approach, aligning with recent research trends, to address the inherent challenges in human-centric anomaly detection.

Regardless of the training methodology employed, human-based VAD is primarily categorized into two strategies: pixel-based (Wang et al., 2023; Zaheer et al., 2022; Georgescu et al., 2021a; Ristea et al., 2022; Wang et al., 2022) and pose-based (Morais et al., 2019; Markovitz et al., 2020; Jain et al., 2021; Rodrigues et al., 2020; Zeng et al., 2021; Yu et al., 2023) methods. For video processing and training, a general technique involves analyzing the pixel data of frames over time. This holds true for VAD as well, where pixel-based approaches examine the raw pixel values in video frames to identify anomalies, leveraging the fine granularity provided by the pixels in each frame. Nonetheless, focusing specifically on human behaviors, the examination of every pixel can result in the analysis of excessive, redundant pixels, introducing undesirable noise into the system (Hirschorn and Avidan, 2023). Such noise can range from relatively harmless disturbances like background changes to more critical issues like demographic attributes (skin color, clothing, gender, etc.), potentially inducing biases within the system. While such noise and biases might not show their effect through available metrics and datasets, they become critical in the deployment of the models in the real world.

Pose-based methods have been developed to mitigate these effects. These methods concentrate

on the poses of individuals within the scene, offering a more refined understanding of human movements (Yu et al., 2023). By prioritizing human poses, these methods not only enhance privacy but also reduce demographic biases and exhibit enhanced resilience against background disturbances, thereby proving their efficacy in diverse real-world applications (Hirschorn and Avidan, 2023; Yu et al., 2023; Alinezhad Noghre et al., 2023). Consequently, this study delves deeper into human pose analysis and leverages it for VAD.

Given the need for self-supervised training and the sequential nature of input pose data transformers emerge as an attractive choice of architecture. Transformers have revolutionized fields such as natural language processing and time series analysis (Li et al., 2022c; Vaswani et al., 2017), are ideally suited for self-supervised learning frameworks (Liu et al., 2023), effectively exploiting the sequential patterns in input data. They excel at capturing long-range dependencies (Khan et al., 2022; Sanford et al., 2024), a crucial attribute for identifying intricate patterns in extensive sequences, such as those encountered in VAD. The challenge, however, lies in adapting the Transformer’s robust attention mechanism to the nuanced requirements of Computer Vision. Here, we aim to bridge this gap by developing a novel tokenization strategy that not only leverages this mechanism but also aligns with the human pose data utilized in our VAD model. This synergy aims to enhance our model’s effectiveness in identifying anomalies in video data while preserving the privacy and bias reduction benefits inherent to pose-centric techniques.

This paper introduces PoseWatch, a novel non-autoregressive transformer-based model with an innovative spatio-temporal tokenization approach for pose-based human-centric anomaly detection. The non-autoregressive design of PoseWatch enables the simultaneous generation of output tokens, crucial for the time-sensitive nature of anomaly detection. Figure 1 provides an abstract overview of the PoseWatch system. PoseWatch features two innovative components: the Spatio-Temporal Pose and Relative Pose (ST-PRP) tokenization and the Unified Encoder Twin Decoders (UETD) transformer core. The ST-PRP tokenization is designed to maximize the self-attention capabilities of the transformer, creating a new paradigm in pose tokenization for a range of

advanced pose-based tasks. The UETD core, with its Future Target Decoder (FTD) and Current Target Decoder (CTD), processes tokens and calculates anomaly scores. This architecture combines a single unified encoder with two decoder heads, each tailored for specific operational goals.

PoseWatch, with just 0.5 million parameters, introduces a self-supervised approach to anomaly detection that sets a new standard for performance across multiple benchmark datasets, including ShanghaiTech (Liu et al., 2018), HR-ShanghaiTech (Morais et al., 2019), and the Charlotte Anomaly Dataset (Danesh Pazho et al., 2023), achieving State-of-the-Art (SotA) average Area Under the Receiver Operating Characteristic Curve (AUC-ROC) score of 80.67%. Additionally, crucial for real-world applications, PoseWatch maintains an impressive average Equal Error Rate (EER) of 0.27, demonstrating SotA balance between false negatives and false positives on these datasets.

This paper presents the following contributions:

- Introducing the Spatio-Temporal Pose and Relative Pose (ST-PRP) tokenization as a novel approach for tokenization of human pose for anomaly detection and showcasing its benefits through extensive ablation study.
- Introducing PoseWatch, the combination of a novel non-autoregressive Unified Encoder Twin Decoders (UETD) transformer and the ST-PRP tokenization, featuring Current Target Decoder (CTD) and Future Target Decoder (FTD) for self-supervised human anomaly detection.
- Demonstrating the accuracy and generalizability of PoseWatch through comparison with not only SotA pose-based approaches but also pixel-based approaches across various benchmark datasets.

2 Related Works

The field of anomaly detection has evolved, adapting to scientific advancements, particularly within the realm of Artificial Intelligence (AI) (Patrikar and Parate, 2022; Zhu et al., 2020). The trend started from handcrafted methods (Coşar et al., 2016; Cheng et al., 2015; Yuan et al., 2014) with approaches utilizing algorithms such as histogram of optical flow (Kaltsa et al., 2015). With the

advancements in deep neural networks, anomaly detection took a leap forward utilizing the learning capabilities of Convolutional Neural Networks (CNNs) (Kong et al., 2021; Sarker et al., 2021; Cheng et al., 2020; Sun et al., 2020; Li et al., 2020). To learn more features, approaches also started adopting Deep Neural Networks (DNNs) (Sabokrou et al., 2017; Suresha et al., 2020; Georgiou et al., 2020; Kim et al., 2021). Long Short-Term Memory was another advancement known for handling time series data. They were widely used in video analysis and surveillance anomaly detection (Ergen and Kozat, 2019; Ullah et al., 2021a,b; Sabih and Vishwakarma, 2022; Asad et al., 2021). Generative Adversarial Networks (GANs) represent another advanced methodology that numerous researchers have adopted for anomaly detection (Jackson and Cuzzolin, 2021; Saypadith and Onoye, 2021; Yang et al., 2021; Zhang et al., 2021; Dong et al., 2020). The most recent approaches have started to leverage transformer architectures (Ullah et al., 2023; Chen et al., 2023b; Li et al., 2022c; Zhang et al., 2022; Huang et al., 2022a; Sun et al., 2022; Madan et al., 2023; Wu et al., 2022) owing to their versatility and deep understanding capabilities enabled by the self-attention module (Vaswani et al., 2017).

There are two main categories for self-supervised human-centric anomaly detection. First are Pixel-based approaches (Barbalau et al., 2023; Madan et al., 2023; Ristea et al., 2022; Li et al., 2022a; Yang et al., 2022) with various subgroups such as Spatio-Temporal Jigsaw Puzzle (Wang et al., 2022), and Multi-Task Design (Georgescu et al., 2021a). Inherently these methods can have an internal bias towards the appearance features of the individuals in the scene as well as high sensitivity towards background noise (Buet-Golfouse and Utyagulov, 2022; Steed and Caliskan, 2021). Like pixel-based approaches, pose-based algorithms can also be divided into multiple subgroups such as methods that use Spatio-Temporal Graph Convolution (Luo et al., 2021), Multi-Scale Prediction (Rodrigues et al., 2020), and Hierarchical Prediction (Zeng et al., 2021).

Normal Graph (Luo et al., 2021) leverages Spatio-Temporal Graph Convolution. When the model, trained only on normal behaviors, predicts future movements that greatly differ from actual

movements, these disparities indicate anomalous behavior. (Rodrigues et al., 2020) employs future and past prediction modules to enhance the accuracy of their anomaly detection model through multi-scale past/future prediction. (Zeng et al., 2021) propose a hierarchical prediction-based method, utilizing three branches to predict pose, trajectory, and motion vectors. MPED-RNN (Morais et al., 2019) and (Li et al., 2022b) employ encoder-decoder structures for anomaly detection utilizing recurrent neural networks. MemWGAN-GP (Li et al., 2023) leverages generative adversarial networks by employing a dual-head decoder structure and upgrading it with a modified version of the Wasserstein Generative Adversarial Network (WGAN-GP) (Arjovsky et al., 2017). GEPC (Markovitz et al., 2020) combines a spatio-temporal graph autoencoder with a clustering layer to assign soft probabilities to input pose segments, serving as an anomaly score. (Yu et al., 2023) incorporates transformers into anomaly detection. This method combines an encoder-only transformer with a simple linear layer as a reconstruction head. STG-NF (Hirschorn and Avidan, 2023) proposes a model that uses normalizing flows to map human pose data distribution to a fixed Gaussian distribution, leveraging spatio-temporal graph convolution blocks. In contrast to all previous methodologies, our approach integrates novel spatio-temporal tokenization, as well as a newly introduced Unified Encoder Twin Decoders transformer core processing, pose through a combination of Current Target Decoder (CTD) and Future Target Decoder (FTD) to achieve the task of human-centric video anomaly detection.

3 PoseWatch

The architecture of PoseWatch, depicted in Figure 2, embodies two main components: the Spatio-Temporal Pose and Relative Pose (ST-PRP) tokenization, alongside the Unified Encoder Twin Decoders (UETD) transformer core. PoseWatch leverages a shared encoder, a Current Target Decode (CTD), and a Future Target Decoder (FTD). The CTD and FTD branches provide complementary insights by capturing distinct patterns within the input sequences. This synergy enhances the overall model’s robustness, as it minimizes the influence of individual branch errors through the

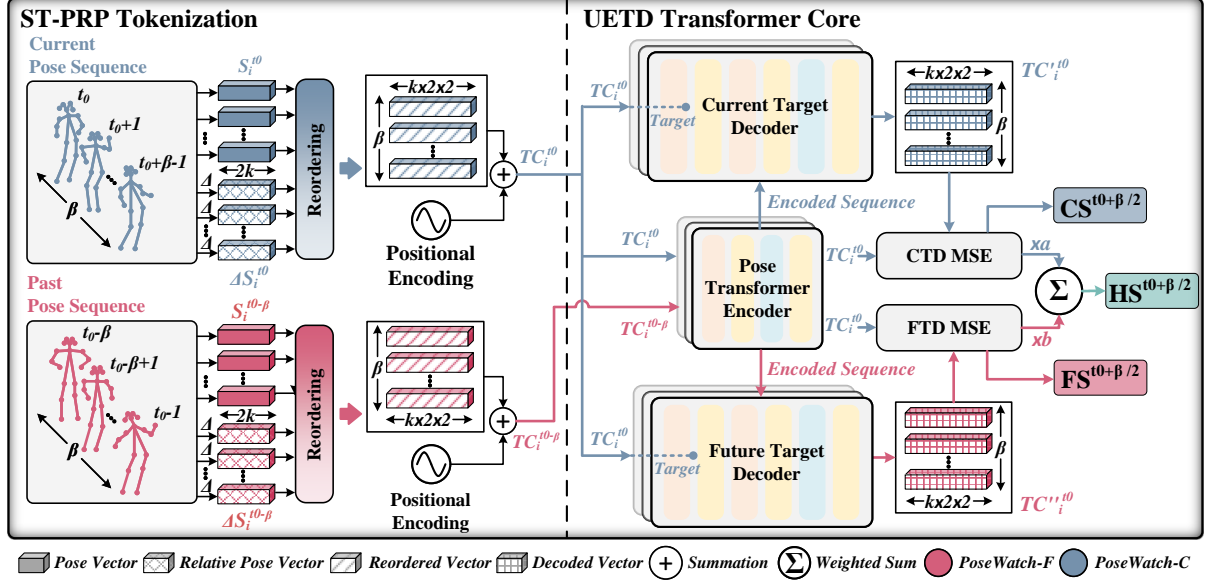


Fig. 2 PoseWatch architecture. ST-PRP tokenization reorders and prepares input pose sequences for being fed to the UETD transformer core. The UETD transformer core consists of a unified pose transformer encoder and twin decoders for CTD and FTD. The MSE loss of both CTD and FTD branches is used to calculate the Current Score (CS) and Future Score (FS), respectively. The average of the two scores is calculated to find the Hybrid Score (HS). Please note that a and b are constant multipliers both set to 0.5 for calculating the HS. Red and blue represent PoseWatch-F and PoseWatch-C data flows respectively.

aggregation of results from both branches. In the following subsections, we delve into the details of Posewatch.

3.1 ST-PRP Tokenization

The tokenization process aims to provide a rich and informative input sequence to the transformer model. We define the absolute pose sequence as follows:

$$S_i^{t_0} = [P_i^{t_0}, P_i^{t_0+1}, P_i^{t_0+2}, \dots, P_i^{t_0+\beta-1}] \quad (1)$$

where S_i is the absolute pose sequence of person i , P is pose data containing (x, y) coordinates of the joints, t_0 is the starting frame of the sequence, and β is the input window size. This will provide the model with basic information about the position of a person's joints in each sequence frame. However, a person's movement patterns through the sequence also reveal critical information for anomaly detection. To accentuate the global movement of humans through space, in addition to the absolute pose sequence, we also leverage the relative pose sequence shown

in Equation (2). ΔS_i is constructed to highlight the overall movements of the subjects relative to the coordinates of the first pose of the current sequence as shown in Equation (3).

$$\Delta S_i^{t_0} = [\Delta P_i^{t_0}, \Delta P_i^{t_0+1}, \Delta P_i^{t_0+2}, \dots, \Delta P_i^{t_0+\beta-1}] \quad (2)$$

$$\Delta P_i^t = P_i^t - P_i^{t_0} \quad (3)$$

ΔP is relative pose data containing relative coordinates of the joints, t_0 is the starting frame of the sequence, and β is the input window size.

The transformer's design exclusively employs inter-token self-attention, ignoring any intra-token attention mechanisms Vaswani et al. (2017). Consequently, the way attention is applied depends significantly on how the input data is tokenized. In order to utilize the full potential of the transformer self-attention module we introduce a Spatio-Temporal Pose and Relative Pose Tokenization (ST-PRP). After conducting extensive experiments with various tokenization strategies, as detailed in Section 6, we identified ST-PRP as the best-performing approach. ST-PRP tokenization, as depicted in Figure 3, employs β tokens,

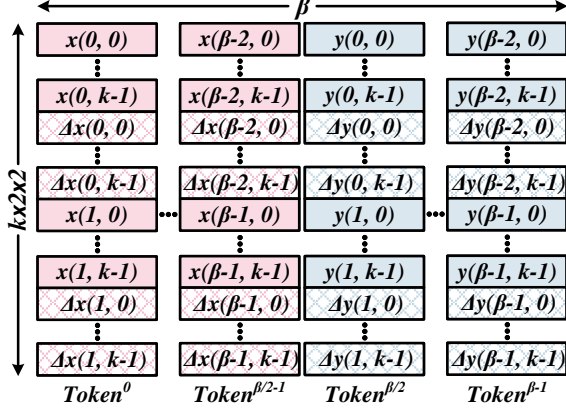


Fig. 3 PoseWatch Spatio-Temporal Pose and Relative Pose (ST-PRP) Tokenization Schema. k is the number of keypoints, β is the input window size, Δ shows relative coordinates and $x(t, k)$ and $y(t, k)$ are the coordinates of k^{th} keypoint in time step t .

each with dimensions of $k \times 2 \times 2$. The initial $\beta/2$ tokens are dedicated to x coordinates, and the latter half pertains to y coordinates. Each token encapsulates both the absolute and relative values of either x or y coordinates of a pose in two adjacent frames. Spatial attention arises from the attention between keypoints and their x and y dimensions, whereas temporal attention is obtained by the frame number progression across tokens. Transformers, by design, do not inherently understand the order of input unless it's explicitly provided. The ST-PRP tokenization captures spatial and temporal relationships within and across frames, but it doesn't inherently indicate the sequence of tokens. Thus, we use the positional encoding strategy (Vaswani et al., 2017) to embed order into the input sequence and construct the input of the PoseWatch Unified Encoder Twin Decoders (UETD) transformer core or TC_i . Further insights into the significance and characteristics of relative pose utilization, along with a detailed analysis of various tokenization methods, through empirical evaluations, are presented in Section 6.

3.2 UETD Transformer Core

At the heart of PoseWatch is the UETD module, which processes tokens generated by the ST-PRP through a dual-branch structure. This core component is trained in a self-supervised manner,

enabling effective anomaly detection. The following sections will go into the details of each of these branches and their architecture.

3.2.1 CTD Branch (PoseWatch-C):

The CTD branch works on the basis that a network trained on the normal data samples in the training set will learn how to encode normal pose sequences to the latent space and generate current sequence with a relatively low Mean Squared Error (MSE) loss. However, if this model is given abnormal pose sequences since it has not seen such datapoints during the training, its generative ability is compromised leading to a relatively larger MSE loss indicating abnormal behavior.

The ST-PRP Tokenization output serves as the input for PoseWatch-C, being treated as a sequential data stream. The PoseWatch CTD branch has an encoder-decoder structure. We chose our design to use a non-autoregressive strategy to take advantage of the parallelization of the transformer's structure. In the CTD branch, we chose the target sequence of the decoder to be equal to the current sequence $TC_i^{t_0}$. Both the encoder and the decoder are chosen to have 12 heads. Considering the real-time nature of the anomaly detection task, we choose a minimal 4 number of layers with the feed-forward layer dimensions set to 64. Unlike most NLP tasks, we do not need to define a start token and end token for the sequences since the input and output sequences have fixed lengths. PoseWatch does not use masking strategies for both the input and target sequences since these sequences are always available even in the inference time. The output of the CTD branch for the input $TC_i^{t_0}$ is:

$$TC_i^{t_0} = [Token_i'^0, Token_i'^1, \dots, Token_i'^{\beta-1}] \quad (4)$$

where $Token_i'^n$ is the n^{th} generated token of the i^{th} person in the t_0 sequence $TC_i^{t_0}$.

Finally, the MSE loss between the generated sequence $TC_i^{t_0}$ and the input sequence $TC_i^{t_0}$ is used both as the training loss and calculating the CTD Score ($CS_i^{t_0+\beta/2}$) in the inference time.

3.2.2 FTD Branch (PoseWatch-F):

As illustrated in Figure 2, the PoseWatch FTD and CTD branches utilize a shared encoder.

This encoder leverages an advanced understanding of pose dynamics and progression when trained for the CTD branch. Correspondingly, the FTD branch employs a decoder mirroring the architecture of the CTD, leveraging 12 heads and 4 layers. Although these decoders have identical architecture (denoted as 'Twin Decoders'), each of them is distinctively tasked. While both generate the current sequence, their inputs differ in timing with FTD's input lagging by one sequence step compared to CTD. Following the non-autoregressive strategy, for the input sequence of $TC_i^{t_0-\beta}$, the target sequence of the decoder is the future sequence ($TC_i^{t_0}$ is considered the future sequence compared to the input of $TC_i^{t_0-\beta}$) in both the training and inferencing process. For the same reason as the CTD branch, We do not use any masking in the FTD branch either. The output of the FTD branch for the input $TC_i^{t_0-\beta}$ is:

$$TC_i''^{t_0} = [Token_i''^0, Token_i''^1, \dots, Token_i''^{\beta-1}] \quad (5)$$

where $Token_i''^n$ is the n^{th} generated token of the i^{th} person in the t_0 sequence $TC_i''^{t_0}$. During the training of this branch, the pose encoder parameters are frozen, and only the FTD decoder parameters are trained. The MSE loss between the generated sequence and the actual sequence is used both for the training process and calculating the FTD Score ($FS_i^{t_0+\beta/2}$) at inference time.

3.2.3 PoseWatch Hybrid (PoseWatch-H):

In order to be able to capture all anomalous patterns detected by both the CTD and the FTD branches, we combine the scores from these branches to calculate the Hybrid Score or HS_i^t of the i^{th} person. We use a weighted sum strategy described in Equation (6). Before combining the scores, we normalize them to ensure they are in the same range.

$$HS_i^{t_0+\frac{\beta}{2}} = 0.5 \cdot Norm(CS_i^{t_0+\frac{\beta}{2}}) + 0.5 \cdot Norm(FS_i^{t_0+\frac{\beta}{2}}) \quad (6)$$

In the last step, we find the maximum anomaly score across all people available in the scene to find one score for each frame:

$$HS^{t_0+\frac{\beta}{2}} = \max_{i \in N} (HS_i^{t_0+\frac{\beta}{2}}) \quad (7)$$

where N is the set of available people in the frame.

In addressing the real-time demands of anomaly detection, our commitment to minimal model complexity is evident, exemplified by only choosing 4 layers for both the encoder and twin decoders. Additionally, diverging from vision transformers employed in various computer vision tasks, our strategy involves tokenized poses with reduced dimensions, resulting in PoseWatch-H only having 0.5 million parameters and an average end-to-end latency of 5.96 ms.

4 Experimental Setup

ShanghaiTech Campus (SHT) (Liu et al., 2018) dataset is the primary benchmark for human-centric video anomaly detection, offering over 317,000 frames from 13 scenes. It includes 274,515 normal training frames and 42,883 test frames with both normal and anomalous events in its unsupervised split. The dataset features unique anomalies as well as various lighting conditions and camera angles, with 130 abnormal events. In line with previous SotA approaches (Markovitz et al., 2020; Hirschorn and Avidan, 2023; Yu et al., 2023), AlphaPose (Li et al., 2019) is utilized for pose extraction and tracking to ensure fair comparison.

HR-ShanghaiTech (HR-SHT) (Morais et al., 2019) represents a human-related adaptation of the SHT dataset. Notably, the only distinction lies in its exclusive focus on human-centric anomalies.

Charlotte Anomaly Dataset (CHAD) (Danesh Pazho et al., 2023) is a new large-scale high-resolution multi-camera VAD dataset with about 1.15 million frames, including 1.09 million normal and 59,172 anomalous frames. Unique for its detailed annotations, including bounding boxes and poses for each subject, CHAD offers a more challenging environment compared to SHT. The experiments are conducted on the unsupervised split. CHAD is selected since it sets a unified benchmark for pose-based anomaly detection by providing extracted poses to eliminate the variations in the final pose-based anomaly detection accuracy.

4.1 Metrics

AUC-ROC or the Area Under the Receiver Operating Characteristic Curve is used to evaluate the discriminative power of models for binary classification. It plots the True Positive Rate (TPR) against the False Positive Rate (FPR) at various thresholds. A higher AUC-ROC value indicates better model performance in class separation.

EER or the Equal Error Rate represents the point at which the False Positive Rate (FPR) and False Negative Rate (FNR) are equal. Owing to the valuable insights that EER provides for anomaly detection, several works such as (Li et al., 2023, 2022b) report it, but it is not used as widely as AUC-ROC. EER finds a balancing point between both error rates, indicating an optimal trade-off between security (inferred from FNR) and usability (inferred from FPR). Notably, EER is not influenced by imbalanced data, which is crucial for anomaly detection problem. On its own, this metric is not informative enough to evaluate a model (Sultani et al., 2018), but in conjunction with AUC-ROC, it provides additional valuable insights (Li et al., 2013).

4.2 Training Strategy and Hyper-parameters

For all the training instances, we employed Adam Optimizer, and the training batch size was set to 256 and 512 for FTD and CTD branches respectively. As for all the training instances dropout rate and weight decay have been set to 0.1 and $5e-5$ respectively. The training procedures were conducted on a workstation equipped with three NVIDIA RTX A6000 graphic cards and an AMD EPYC 7513 32-core processor. A conventional grid hyper-parameter search was systematically utilized to find the optimal set of hyper-parameters.

SHT (Liu et al., 2018) has been recorded at 24 FPS. Thus, we consider the input sequence length to be 24, equivalent to 1s. PoseWatch-C underwent training for 20 epochs with a learning rate of $1e-5$. In the next step, we freeze the parameters of the trained pose encoder and train the PoseWatch-F decoder for 30 epochs with a learning rate of $2e-3$.

HR-SHT (Morais et al., 2019) contains the same videos in the training set as SHT. Thus, we do not have a separate training for it. We use the

model trained on SHT and validate it on the HR-SHT subset as well.

CHAD (Danesh Pazho et al., 2023) is recorded at 30 FPS. Thus, we chose the input sequence length to be 1s or 30 frames. PoseWatch-C is trained for 30 epochs with a learning rate of $2e-3$. In the next step, We freeze the parameters of the pose encoder and train the PoseWatch-F decoder for 30 epochs with a learning rate of $5e-4$.

The training approach is entirely self-supervised, identifying the best model through the minimization of MSE loss on the training data. This model is then subjected to a single evaluation on the test set to assess its anomaly detection efficacy.

5 Results

5.1 Comparison With Pose-based Approaches

Table 1 presents the performance of PoseWatch and its variants on three distinct datasets: SHT (Liu et al., 2018), HR-SHT (Morais et al., 2019), and CHAD (Danesh Pazho et al., 2023). Unfortunately, most works do not provide their code base for further examinations on the newer dataset.

Table 1 AUC-ROC of PoseWatch compared with pose-based approaches on SHT (Liu et al., 2018), HR-SHT (Morais et al., 2019), and CHAD (Danesh Pazho et al., 2023) datasets. PoseWatch is compared to SotA methods such as MPED-RNN (Morais et al., 2019), GEPC (Markovitz et al., 2020), PoseCVAE (Jain et al., 2021), MSTA-GCN (Chen et al., 2023a), MTP (Rodrigues et al., 2020), HSTGCNN (Zeng et al., 2021), STGformer Huang et al. (2022b), MoPRL (Yu et al., 2023) and STG-NF (Hirschorn and Avidan, 2023). The best is in bold and the second best is underlined.

Methods	SHT	HR-SHT	CHAD	Average
MPED-RNN	73.40	75.40	-	-
GEPC	75.50	-	64.90	-
PoseCVAE	74.90	75.70	-	-
MSTA-GCN	75.90	-	-	-
MTP	76.03	77.04	-	-
HSTGCNN	81.80	83.40	-	-
STGformer	82.90	86.97	-	-
MoPRL	83.35	84.40	-	-
STG-NF	85.90	87.40	60.60	78.63
PoseWatch-C	85.10	86.70	<u>66.12</u>	<u>79.31</u>
PoseWatch-F	83.19	83.70	66.61	77.17
PoseWatch-H	<u>85.75</u>	<u>87.23</u>	67.04	80.67

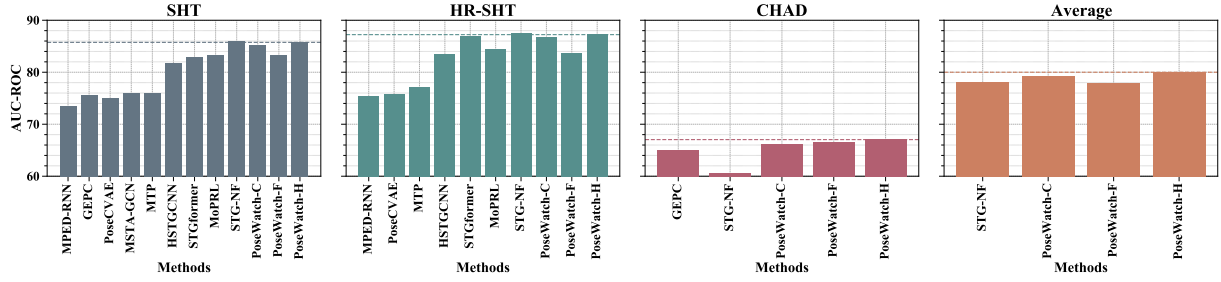


Fig. 4 AUC-ROC of PoseWatch compared with pose-based approaches on SHT (Liu et al., 2018), HR-SHT (Morais et al., 2019), and CHAD (Danesh Pazho et al., 2023) datasets. PoseWatch is compared to MPED-RNN (Morais et al., 2019), GEPC (Markovitz et al., 2020), PoseCVAE (Jain et al., 2021), MSTA-GCN (Chen et al., 2023a), MTP (Rodrigues et al., 2020), HSTGCNN (Zeng et al., 2021), STGformer (Huang et al., 2022b), MoPRL (Yu et al., 2023) and STG-NF (Hirschorn and Avidan, 2023). The best results of PoseWatch is demonstrated using dashed lines per each dataset. The average is only calculated for algorithms with results for all three datasets for fairness. Detailed numbers can be seen in Table 1.

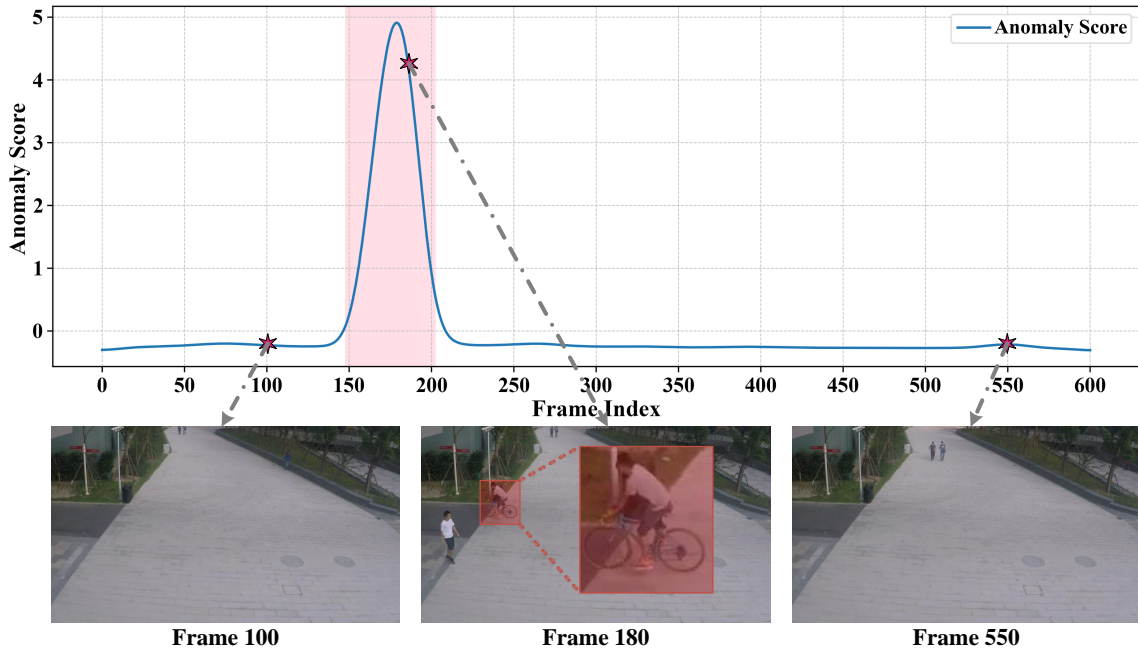


Fig. 5 Output anomaly scores of PoseWatch-H for each frame of clip 01_0025 from the SHT dataset (Liu et al., 2018). The red area on the plot indicates the ground truth anomalous frames. In this clip, the anomalous behavior is a person riding a bike on the sidewalk shown by the red rectangle.

Based on Table 1 and Figure 4 PoseWatch-H establishes itself as the most accurate model for VAD with an average AUC-ROC that surpasses the previous state-of-the-art by 2.04%, as demonstrated across three benchmark datasets. Specifically, on the CHAD dataset, PoseWatch-H outperforms the prior best model by 2.14%, highlighting its robustness in complex environments.

On the SHT and HR-SHT datasets, PoseWatch-H secures the second-highest AUC-ROC scores of 85.75% and 87.23%, respectively, trailing STG-NF by only 0.15% and 0.17%. However, STG-NF’s approach, which relies on probabilistic modeling with a fixed normal distribution, limits its generalizability, particularly on the diverse CHAD dataset, where it underperforms by 6.44%. This

Table 2 EER of PoseWatch compared with pose-based approaches on SHT (Liu et al., 2018), HR-SHT (Morais et al., 2019), and CHAD (Danesh Pazho et al., 2023) datasets. PoseWatch is compared to SotA methods such as GEPC (Markovitz et al., 2020) and STG-NF (Hirschorn and Avidan, 2023). The best is in bold and the second best is underlined.

Methods	SHT	HR-SHT	CHAD	Average
GEPC	0.31	-	<u>0.38</u>	-
STG-NF	0.22	0.21	0.43	0.29
PoseWatch-C	<u>0.23</u>	<u>0.22</u>	<u>0.38</u>	<u>0.28</u>
PoseWatch-F	0.25	0.25	<u>0.38</u>	0.29
PoseWatch-H	0.22	0.21	0.37	0.27

shortfall underscores PoseWatch-H’s superior ability to model diverse normal scenarios, making it the most effective model overall. Additionally, PoseWatch-C, which ranks second in average AUC-ROC, further demonstrates the effectiveness and versatility of the PoseWatch approach, solidifying its position as a new standard in pose-based VAD.

Examining the EER across all datasets, Table 2 reveals that PoseWatch-H consistently outperforms previous SotA, with an average EER of 0.27 compared to STG-NF’s 0.29. This trend mirrors the AUC-ROC results, further solidifying PoseWatch-H as the superior model in terms of overall performance and generalizability. Both PoseWatch-H and STG-NF achieve an EER of 0.22 on the SHT dataset. However, the CHAD dataset underscores the limitations of STG-NF, where it shows a higher EER of 0.43 compared to PoseWatch-H’s lower EER of 0.37. This difference highlights PoseWatch-H’s broader applicability and robustness across diverse datasets, making it a more versatile solution, especially for real-world applications where balancing false positive rates (usability) and false negative rates (security) is crucial.

In the comparison of PoseWatch-H with its variants, namely PoseWatch-C and PoseWatch-F, as depicted in Table 1, it is evident that PoseWatch-H consistently demonstrates superior performance when compared to its counterparts. For instance, in the SHT dataset, PoseWatch-C and PoseWatch-F register AUC-ROC scores of 85.10% and 83.19%, respectively, whereas PoseWatch-H surpasses them with an AUC-ROC of 85.75% and 87.23%. This enhancement in performance is attributed to the synergistic effect of

integrating CTD and FTD branches. It shows that the CTD alone may miss certain anomalies, which the FTD can detect, and vice versa. This complementary relationship is not limited to AUC-ROC; similar trends are observed in EER measurements, shown in Table 2, further underscoring the robustness of PoseWatch-H compared to its individual sub-branches. Despite the lower AUC-ROC values and higher EER metrics observed in PoseWatch-C and PoseWatch-F relative to PoseWatch-H, these models still demonstrate competitive performance when benchmarked against other SotA methodologies, as evidenced in Table 2.

Table 3 AUC-ROC of PoseWatch compared with pixel-based approaches on SHT (Liu et al., 2018) and HR-SHT (Morais et al., 2019) datasets. PoseWatch is compared with SotA methods such as MAAM-Net (Wang et al., 2023), GCL_{PT} (Zaheer et al., 2022), BAF (Georgescu et al., 2021b), BAF (Georgescu et al., 2021b) + SSPCAB (Ristea et al., 2022), SSMTL (Georgescu et al., 2021a), SSMTL++v2 (Barbalau et al., 2023), Jigsaw-VAD (Wang et al., 2022) and NM-GAN (Chen et al., 2021). The best is in bold and the second best is underlined.

Methods	SHT	HR-SHT	Average
MAAM-Net	71.30	-	-
GCL _{PT}	78.93	-	-
BAF	82.70	-	-
BAF + SSPCAB	83.60	-	-
SSMTL	83.50	-	-
SSMTL++v2	83.80	-	-
Jigsaw-VAD	84.30	84.70	84.50
NM-GAN	<u>85.30</u>	-	-
PoseWatch-C	85.10	<u>86.70</u>	<u>85.90</u>
PoseWatch-F	83.19	83.70	83.45
PoseWatch-H	85.75	87.23	86.49

To further illustrate the effectiveness of the proposed model, two examples from SHT (Liu et al., 2018) and CHAD (Danesh Pazho et al., 2023) are shown in Figure 5 and Figure 6. The y-axis represents the output anomaly score of PoseWatch-H for all frames of the testing clip. As depicted in Figure 5, PoseWatch-H accurately detects anomalous behavior, maintaining a steady score on normal frames and showing an increased score on anomalous ones. Figure 6 similarly demonstrates that PoseWatch-H produces higher scores for anomalous frames, enabling anomaly detection. However, more noise is evident in Figure 6, and it is not as accurate as in Figure 5,

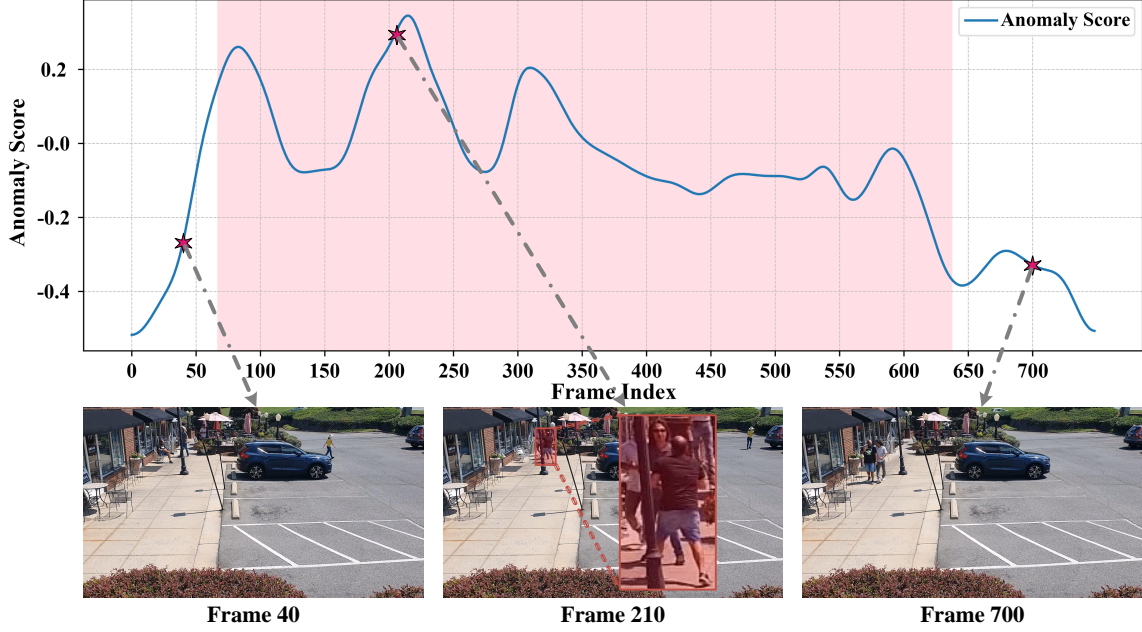


Fig. 6 Output anomaly scores of PoseWatch-H for each frame of clip 04_093.1 from the CHAD dataset (Danesh Pazho et al., 2023). The red area on the plot indicates the ground truth anomalous frames. In this clip, the anomalous behavior is two people fighting shown by the red rectangle.

which is also reflected by the lower AUC-ROC and higher EER observed on the CHAD dataset compared to the SHT dataset showcased in Table 1 and Table 2.

5.2 Comparison With Pixel-based Approaches

This manuscript mainly focuses on pose-based approaches. However, we will further explore an additional comparative analysis between PoseWatch and pixel-based methodologies to have a better understanding of PoseWatch’s capabilities. The datasets common between pose-based and pixel-based approaches are SHT (Liu et al., 2018) and with one reported instance (Wang et al., 2022), HR-SHT (Morais et al., 2019). Notably, CHAD has not yet been employed in pixel-based studies. Therefore, we further compare PoseWatch with SotA pixel-based algorithms on SHT and HR-SHT.

As outlined in Section 1 and Section 2, pixel-based approaches have historically been regarded as more precise than pixel-based approaches. Nonetheless, recent studies indicate a shift in

this trend. In Table 3, we present a comparative analysis of PoseWatch against current SotA pixel-based algorithms. PoseWatch-H achieves an average AUC-ROC of 86.49% across the SHT and HR-SHT datasets, underscoring its overall superiority. Notably, PoseWatch-H demonstrates superior performance with AUC-ROC scores of 85.75% and 87.23% on the SHT and HR-SHT datasets, respectively. This superior performance is noteworthy considering that PoseWatch is a pose-based approach. This approach inherently exhibits lower bias and reduced susceptibility to background noise, while simultaneously promoting greater privacy and adhering to ethical standards. Furthermore, despite processing less information than its pixel-based counterparts, PoseWatch-H consistently achieves higher AUC-ROC.

6 Ablation Study

6.1 Impact of Relative Pose

The results detailed in Table 4 empirically validate the effectiveness of using relative pose tokenization, as theoretically outlined in Section 3.1. This

Table 4 Evaluating AUC-ROC of PoseWatch on SHT (Liu et al., 2018), HR-SHT (Morais et al., 2019), and CHAD (Daneshe Pazho et al., 2023) datasets: A comparative analysis of our design variants with and without incorporating relative motion. The best result of each branch is highlighted in gray.

	Relative Movement	SHT	HR-SHT	CHAD
PoseWatch-C	✗	82.97	84.80	57.56
	✓	85.10	86.70	66.12
PoseWatch-F	✗	81.80	82.80	58.27
	✓	83.19	83.70	66.61
PoseWatch-H	✗	84.20	85.47	57.95
	✓	85.75	87.23	67.04

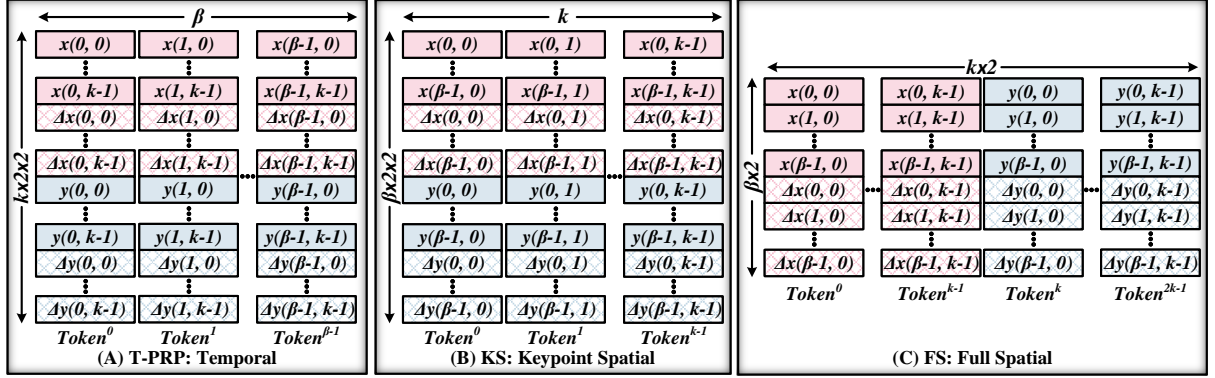


Fig. 7 Proposed tokenization methods. k is the number of keypoints, β is the input window size, Δ shows relative coordinates and $x(t, k)$ and $y(t, k)$ are the coordinates of k^{th} keypoint in time step t .

empirical evidence complements and reinforces the theory that incorporating global movement benefits anomaly detection. The results indicate a consistent improvement across all three variations of the PoseWatch when the relative pose is integrated. Specifically, regarding AUC-ROC, the PoseWatch-H variant incorporating relative movement demonstrates a notable performance enhancement. On the SHT dataset, for instance, the use of relative movement in PoseWatch-H results in an AUC-ROC increase of 1.55% compared to its counterpart without relative movement. This improvement is even more pronounced in the CHAD, where PoseWatch-H with relative movement achieves a 9.09% higher AUC-ROC than the version without relative pose integration. These findings underscore the significant impact of relative pose tokenization on the model’s results.

6.2 Exploring Diverse Tokenization Strategies

We employed diverse tokenization strategies to optimize the synergy between temporal and spatial attention. This experiment aims to identify the most effective method for the transformer core to interpret and analyze pose behavior more accurately, optimizing its overall anomaly detection capabilities. The input window of size β and the number of keypoints k remain consistent across all implemented strategies, ensuring a uniform basis for comparability. For each tokenization method, the best model was selected after a grid hyperparameter search; details can be found in the supplementary materials.

Temporal Pose and Relative Pose (T-PRP) tokenization prioritizes the temporal motion between video frames by encapsulating the information of an individual frame, encompassing its pose and relative pose represented as (x, y) and $(\Delta x, \Delta y)$ coordinates, within a single token -

Table 5 Evaluating AUC-ROC of PoseWatch on SHT (Liu et al., 2018), HR-SHT (Morais et al., 2019), and CHAD (Danesh Pazho et al., 2023) datasets: A comparative analysis of our design with different methods of tokenization. The best result of each branch is highlighted in gray.

	Tokenization	SHT	HR-SHT	CHAD
PoseWatch-C	T-PRP	83.85	85.46	65.59
	KS-PRP	83.67	85.15	64.69
	FS-PRP	83.45	85.13	62.84
	ST-PRP	85.10	86.70	66.12
PoseWatch-F	T-PRP	82.08	84.47	66.18
	KS-PRP	79.53	80.40	64.95
	FS-PRP	82.08	83.21	64.29
	ST-PRP	83.19	83.70	66.61
PoseWatch-H	T-PRP	84.40	86.06	67.06
	KS-PRP	83.63	84.94	65.37
	FS-PRP	84.68	86.37	64.28
	ST-PRP	85.75	87.23	67.04

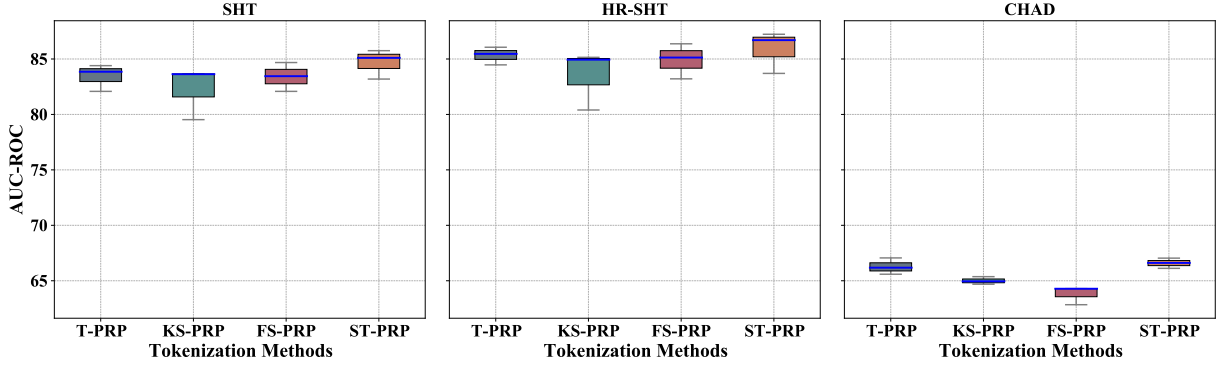


Fig. 8 Box and Whiskers of various tokenization methods and their effectiveness with regards to AUC-ROC over SHT (Liu et al., 2018), HR-SHT (Morais et al., 2019), and CHAD (Danesh Pazho et al., 2023) datasets. The plots clearly demonstrate the superiority of the ST-PRP method, which outperforms all other tokenization methodologies across all tested datasets.

underscoring the sequential nature of the frames. As depicted in Figure 7 part (A) each token has dimensions of $k \times 2 \times 2$ and the number of tokens matches the window size β .

Keypoint Spatial Pose and Relative Pose (KS-PRP) tokenization focuses on the interrelation among keypoints within a sequence of poses. As illustrated in Figure 7 (B), each token encapsulates the positional information of a specific keypoint (e.g., elbow) in terms of x and y coordinates across all frames within the input window. Consequently, the size of each token is $\beta \times 2 \times 2$. This creates k input tokens, each representing one of the k^{th} keypoints.

Full Spatial Pose and Relative Pose (FS-PRP) tokenization, similar to KP tokenization,

also focuses on the relationship between the keypoints of a pose, it takes into account that there is a relationship between the x and y of a certain keypoint (e.g. elbow) too. Consequently, FS tokenization refines the tokenization scheme of KS tokenization further by partitioning x and y coordinates, thereby creating $k \times 2$ tokens. The initial set of k tokens pertains to x coordinates, while the subsequent set of k tokens pertains to y coordinates.

On top of all these tokenization strategies, we also add positional encoding to embed order into input sequences. In Table 5, the performance of various tokenization methods is compared. The ST-PRP tokenization method, detailed in Section 3.1, demonstrates superior performance in most cases compared to other approaches. While

the T-PRP tokenization outperforms others in two specific instances, purely spatial tokenizations (KS-PRP and FS-PRP) consistently yield sub-optimal results. Figure 8 further supports this observation, clearly demonstrating that across all three benchmark datasets, the PoseWatch variants achieve higher overall AUC-ROC when using ST-PRP tokenization. This suggests that the combination of temporal and spatial attention between tokens uncovers crucial information for analyzing human behavior patterns that neither can detect independently. Consequently, the ST tokenization method, which integrates spatial and temporal information, emerges as the most effective approach.

7 Conclusion

In this paper, we introduced methodologies that pave the way for advanced human-centric Video Anomaly Detection (VAD). The novel proposed Spatio-Temporal Pose and Relative Pose (ST-PRP) tokenization method, which serves as a key component for high-level human behavior analysis. Combined with our new Unified Encoder Twin Decoders (UETD) transformer core, the proposed PoseWatch architecture demonstrates superior performance in self-supervised human-centric VAD. Extensive benchmarking against SotA methods confirms PoseWatch’s accuracy and robustness. We hope that our contributions will serve as a foundation for future advancements in the field.

Appendix A Ablation Studies Hyperparameters

This section provides an in-depth exposition of the architectural and training hyperparameters of the ablation studies (Section 6). It is aimed at ensuring reproducibility of the results.

A.1 Relative Pose Ablation Setup and Hyperparameters

To reveal the benefit of incorporating relative movement, we use the best PoseWatch model which includes 12 heads and 4 layers with the feed-forward layer size set to 64. This variant is

Table A1 The training hyperparameters used for the Relative Pose Ablation Study (Section 6.1) on SHT (Liu et al., 2018), HR-SHT (Morais et al., 2019) and CHAD (Danesh Pazho et al., 2023) datasets. LR and DR refer to the Learning Rate and Dropout Rate.

		SHT, HR-SHT		CHAD	
	Relative Movement	LR	DR	LR	DR
PoseWatch-C	\times \checkmark	$2.0e-3$ $1.0e-5$	0.1 0.1	$5.0e-6$ $2.0e-3$	0.1 0.1
PoseWatch-F	\times \checkmark	$5.0e-4$ $2.0e-3$	0.1 0.1	$3.0e-3$ $5.0e-4$	0.1 0.1

Table A2 The design choices used for the Tokenization Ablation Study (Section 6.2)

	# Heads	# Layers	Feed Forward Dimension
T-PRP	8	8	128
KS-PRP	8	4	128
FS-PRP	12	6	64
ST-PRP	12	4	64

trained with and without relative movement data using the hyperparameters shown in Table A1. The optimal hyperparameters are chosen using a systematic grid search. In all training instances, we have used the Adam optimizer with a weight decay of $5.0e-5$ and trained branches for 30 epochs. For the training, the same strategy is used as in Section 4 in the original manuscript; first, the PoseWatch-C (the unified encoder and CTD decoder) is trained. In the next step, the unified encoder is frozen and the FTD decoder is trained. Since both the SHT and HR-SHT utilize identical videos in their training sets, the hyperparameters for both models remain consistent.

A.2 Tokenization Ablation Setup and Hyperparameters

To effectively compare various tokenization setups, we carried out a systematic grid search. This approach was not just to identify the optimal training hyperparameters, but also to determine the best architectural choices. This thorough process ensures that each tokenization setup is evaluated at its highest potential, leading to more accurate and reliable comparison results.

Table A2 presents the architectural design parameter choices obtained from the grid search on SHT dataset (Liu et al., 2018). These parameters are kept the same for other datasets to

Table A3 The training hyperparameters used for the Tokenization Ablation Study (Section 6.2) on SHT (Liu et al., 2018), HR-SHT (Morais et al., 2019) and CHAD (Danesh Pazho et al., 2023) datasets. LR and DR refer to the Learning Rate and Dropout Rate.

		SHT, HR-SHT		CHAD	
		LR	DR	LR	DR
PoseWatch-C	T-PRP	$5.0e-6$	0.1	$3.0e-3$	0.1
	KS-PRP	$5.0e-6$	0.1	$3.0e-3$	0.2
	FS-PRP	$1.0e-5$	0.1	$1.0e-3$	0.1
	ST-PRP	$1.0e-5$	0.1	$2.0e-3$	0.1
PoseWatch-F	T-PRP	$3.0e-3$	0.1	$1.0e-4$	0.1
	KS-PRP	$1.0e-4$	0.2	$1.0e-4$	0.1
	FS-PRP	$5.0e-4$	0.1	$1.0e-5$	0.1
	ST-PRP	$2.0e-3$	0.1	$5.0e-4$	0.1

ensure a fair comparison. Across all experiments, both the unified encoder and the twin decoders consistently adhere to the parameters detailed in Table A2. This consistency ensures a standardized approach in our experimental setup. On the other hand, Table A3 shows the best learning rate and dropout for training per branch. The number of epochs, optimizer, and weight decay are 30, Adam, and $5.0e-5$ respectively.

Regarding the training process, same as other tests, PoseWatch-C is initially trained following the strategy outlined in Section 4.2 in the original manuscript, where both the unified encoder and the CTD decoder are trained together. Subsequently, for PoseWatch-F, the unified encoder is frozen, and then only the FTD decoder undergoes further training. As the training sets for both the SHT and HR-SHT consist of the same videos, the hyperparameters are kept uniform for them.

References

Abbas, Z. K. and Al-Ani, A. A. (2022). A comprehensive review for video anomaly detection on videos. In *2022 International Conference on Computer Science and Software Engineering (CSASE)*, pages 1–1. IEEE.

Alinezhad Noghre, G., Danesh Pazho, A., Katariya, V., and Tabkhi, H. (2023). Understanding the challenges and opportunities of pose-based anomaly detection. In *Proceedings of the 8th international Workshop on Sensor-Based Activity Recognition and Artificial Intelligence*, pages 1–9.

Arjovsky, M., Chintala, S., and Bottou, L. (2017). Wasserstein generative adversarial networks. In

Precup, D. and Teh, Y. W., editors, *Proceedings of the 34th International Conference on Machine Learning*, volume 70 of *Proceedings of Machine Learning Research*, pages 214–223. PMLR.

Asad, M., Yang, J., He, J., Shamsolmoali, P., and He, X. (2021). Multi-frame feature-fusion-based model for violence detection. *The Visual Computer*, 37:1415–1431.

Barbalau, A., Ionescu, R. T., Georgescu, M.-I., Dueholm, J., Ramachandra, B., Nasrollahi, K., Khan, F. S., Moeslund, T. B., and Shah, M. (2023). Ssm1++: Revisiting self-supervised multi-task learning for video anomaly detection. *Computer Vision and Image Understanding*, 229:103656.

Buet-Golfouse, F. and Utyagulov, I. (2022). Towards fair unsupervised learning. In *Proceedings of the 2022 ACM Conference on Fairness, Accountability, and Transparency*, pages 1399–1409.

Chen, D., Yue, L., Chang, X., Xu, M., and Jia, T. (2021). Nm-gan: Noise-modulated generative adversarial network for video anomaly detection. *Pattern Recognition*, 116:107969.

Chen, X., Kan, S., Zhang, F., Cen, Y., Zhang, L., and Zhang, D. (2023a). Multiscale spatial temporal attention graph convolution network for skeleton-based anomaly behavior detection. *Journal of Visual Communication and Image Representation*, 90:103707.

Chen, Y., Liu, Z., Zhang, B., Fok, W., Qi, X., and Wu, Y.-C. (2023b). Mgnf: Magnitude-contrastive glance-and-focus network for weakly-supervised video anomaly detection. In *Proceedings of the AAAI Conference on Artificial Intelligence*, volume 37, pages 387–395.

Cheng, H., Liu, X., Wang, H., Fang, Y., Wang, M., and Zhao, X. (2020). Securead: A secure video anomaly detection framework on convolutional neural network in edge computing environment. *IEEE Transactions on Cloud Computing*, 10(2):1413–1427.

Cheng, K.-W., Chen, Y.-T., and Fang, W.-H. (2015). Gaussian process regression-based video anomaly detection and localization with hierarchical feature representation. *IEEE Transactions on Image Processing*, 24(12):5288–5301.

- Coşar, S., Donatiello, G., Bogorny, V., Garate, C., Alvares, L. O., and Brémond, F. (2016). Toward abnormal trajectory and event detection in video surveillance. *IEEE Transactions on Circuits and Systems for Video Technology*, 27(3):683–695.
- Danesh Pazho, A., Alinezhad Noghre, G., Rahimi Ardabili, B., Neff, C., and Tabkhi, H. (2023). Chad: Charlotte anomaly dataset. In *Scandinavian Conference on Image Analysis*, pages 50–66. Springer.
- Dong, F., Zhang, Y., and Nie, X. (2020). Dual discriminator generative adversarial network for video anomaly detection. *IEEE Access*, 8:88170–88176.
- Ergen, T. and Kozat, S. S. (2019). Unsupervised anomaly detection with lstm neural networks. *IEEE transactions on neural networks and learning systems*, 31(8):3127–3141.
- Georgescu, M.-I., Barbalau, A., Ionescu, R. T., Khan, F. S., Popescu, M., and Shah, M. (2021a). Anomaly detection in video via self-supervised and multi-task learning. In *Proceedings of the IEEE/CVF conference on computer vision and pattern recognition*, pages 12742–12752.
- Georgescu, M. I., Ionescu, R. T., Khan, F. S., Popescu, M., and Shah, M. (2021b). A background-agnostic framework with adversarial training for abnormal event detection in video. *IEEE transactions on pattern analysis and machine intelligence*, 44(9):4505–4523.
- Georgiou, T., Liu, Y., Chen, W., and Lew, M. (2020). A survey of traditional and deep learning-based feature descriptors for high dimensional data in computer vision. *International Journal of Multimedia Information Retrieval*, 9(3):135–170.
- Hirschorn, O. and Avidan, S. (2023). Normalizing flows for human pose anomaly detection. In *Proceedings of the IEEE/CVF International Conference on Computer Vision*, pages 13545–13554.
- Huang, C., Liu, C., Wen, J., Wu, L., Xu, Y., Jiang, Q., and Wang, Y. (2022a). Weakly supervised video anomaly detection via self-guided temporal discriminative transformer. *IEEE Transactions on Cybernetics*.
- Huang, C., Liu, Y., Zhang, Z., Liu, C., Wen, J., Xu, Y., and Wang, Y. (2022b). Hierarchical graph embedded pose regularity learning via spatio-temporal transformer for abnormal behavior detection. In *Proceedings of the 30th ACM International Conference on Multimedia*, pages 307–315.
- Jackson, S. D. and Cuzzolin, F. (2021). Svd-gan for real-time unsupervised video anomaly detection. In *Proceedings of the British Machine Vision Conference (BMVC), Virtual*, pages 22–25.
- Jain, Y., Sharma, A. K., Velmurugan, R., and Banerjee, B. (2021). Posecvae: Anomalous human activity detection. In *2020 25th International Conference on Pattern Recognition (ICPR)*, pages 2927–2934. IEEE.
- Kaltsa, V., Briassouli, A., Kompatsiaris, I., Hadjileontiadis, L. J., and Strintzis, M. G. (2015). Swarm intelligence for detecting interesting events in crowded environments. *IEEE transactions on image processing*, 24(7):2153–2166.
- Khan, S., Naseer, M., Hayat, M., Zamir, S. W., Khan, F. S., and Shah, M. (2022). Transformers in vision: A survey. *ACM computing surveys (CSUR)*, 54(10s):1–41.
- Kim, J.-H., Kim, N., and Won, C. S. (2021). Deep edge computing for videos. *IEEE Access*, 9:123348–123357.
- Kong, X., Wang, K., Wang, S., Wang, X., Jiang, X., Guo, Y., Shen, G., Chen, X., and Ni, Q. (2021). Real-time mask identification for covid-19: An edge-computing-based deep learning framework. *IEEE Internet of Things Journal*, 8(21):15929–15938.
- Li, G., Cai, G., Zeng, X., and Zhao, R. (2022a). Scale-aware spatio-temporal relation learning for video anomaly detection. In *European Conference on Computer Vision*, pages 333–350. Springer.
- Li, J., Wang, C., Zhu, H., Mao, Y., Fang, H.-S., and Lu, C. (2019). Crowdpose: Efficient crowded scenes pose estimation and a new benchmark. In *Proceedings of the IEEE/CVF conference on computer vision and pattern recognition*, pages 10863–10872.
- Li, N., Chang, F., and Liu, C. (2022b). Human-related anomalous event detection via spatial-temporal graph convolutional autoencoder with embedded long short-term memory network. *Neurocomputing*, 490:482–494.
- Li, N., Chang, F., and Liu, C. (2023). Human-related anomalous event detection via memory-augmented wasserstein generative adversarial

- network with gradient penalty. *Pattern Recognition*, 138:109398.
- Li, S., Liu, F., and Jiao, L. (2022c). Self-training multi-sequence learning with transformer for weakly supervised video anomaly detection. In *Proceedings of the AAAI Conference on Artificial Intelligence*, volume 36, pages 1395–1403.
- Li, W., Mahadevan, V., and Vasconcelos, N. (2013). Anomaly detection and localization in crowded scenes. *IEEE transactions on pattern analysis and machine intelligence*, 36(1):18–32.
- Li, Z., Li, Y., and Gao, Z. (2020). Spatiotemporal representation learning for video anomaly detection. *IEEE Access*, 8:25531–25542.
- Liu, W., Luo, W., Lian, D., and Gao, S. (2018). Future frame prediction for anomaly detection—a new baseline. In *Proceedings of the IEEE conference on computer vision and pattern recognition*, pages 6536–6545.
- Liu, Y., Zhang, Y., Wang, Y., Hou, F., Yuan, J., Tian, J., Zhang, Y., Shi, Z., Fan, J., and He, Z. (2023). A survey of visual transformers. *IEEE Transactions on Neural Networks and Learning Systems*.
- Luo, W., Liu, W., and Gao, S. (2021). Normal graph: Spatial temporal graph convolutional networks based prediction network for skeleton based video anomaly detection. *Neurocomputing*, 444:332–337.
- Madan, N., Ristea, N.-C., Ionescu, R. T., Nasrollahi, K., Khan, F. S., Moeslund, T. B., and Shah, M. (2023). Self-supervised masked convolutional transformer block for anomaly detection. *IEEE Transactions on Pattern Analysis and Machine Intelligence*.
- Markovitz, A., Sharir, G., Friedman, I., Zelnik-Manor, L., and Avidan, S. (2020). Graph embedded pose clustering for anomaly detection. In *Proceedings of the IEEE/CVF Conference on Computer Vision and Pattern Recognition*, pages 10539–10547.
- Morais, R., Le, V., Tran, T., Saha, B., Mansour, M., and Venkatesh, S. (2019). Learning regularity in skeleton trajectories for anomaly detection in videos. In *Proceedings of the IEEE/CVF conference on computer vision and pattern recognition*, pages 11996–12004.
- Nanda, S. K., Ghai, D., Ingole, P., and Pande, S. (2022). Soft computing techniques-based digital video forensics for fraud medical anomaly detection. *Computer Assisted Methods in Engineering and Science*, 30(2):111–130.
- Patrikar, D. R. and Parate, M. R. (2022). Anomaly detection using edge computing in video surveillance system. *International Journal of Multimedia Information Retrieval*, 11(2):85–110.
- Pazho, A. D., Neff, C., Noghre, G. A., Ardabili, B. R., Yao, S., Baharani, M., and Tabkhi, H. (2023). Ancilia: Scalable intelligent video surveillance for the artificial intelligence of things. *IEEE Internet of Things Journal*.
- Pazho, A. D., Noghre, G. A., Katariya, V., and Tabkhi, H. (2024). Vt-former: An exploratory study on vehicle trajectory prediction for highway surveillance through graph isomorphism and transformer. In *Proceedings of the IEEE/CVF Conference on Computer Vision and Pattern Recognition (CVPR) Workshops*, pages 5651–5662.
- Ramachandra, B., Jones, M. J., and Vatsavai, R. R. (2020). A survey of single-scene video anomaly detection. *IEEE transactions on pattern analysis and machine intelligence*, 44(5):2293–2312.
- Ren, J., Xia, F., Liu, Y., and Lee, I. (2021). Deep video anomaly detection: Opportunities and challenges. In *2021 international conference on data mining workshops (ICDMW)*, pages 959–966. IEEE.
- Ristea, N.-C., Madan, N., Ionescu, R. T., Nasrollahi, K., Khan, F. S., Moeslund, T. B., and Shah, M. (2022). Self-supervised predictive convolutional attentive block for anomaly detection. In *Proceedings of the IEEE/CVF conference on computer vision and pattern recognition*, pages 13576–13586.
- Rodrigues, R., Bhargava, N., Velmurugan, R., and Chaudhuri, S. (2020). Multi-timescale trajectory prediction for abnormal human activity detection. In *Proceedings of the IEEE/CVF Winter Conference on Applications of Computer Vision*, pages 2626–2634.
- Sabih, M. and Vishwakarma, D. K. (2022). Crowd anomaly detection with lstms using optical features and domain knowledge for improved inferring. *The Visual Computer*, 38(5):1719–1730.
- Sabokrou, M., Fayyaz, M., Fathy, M., and Klette, R. (2017). Deep-cascade: Cascading 3d deep neural networks for fast anomaly detection and

- localization in crowded scenes. *IEEE Transactions on Image Processing*, 26(4):1992–2004.
- Sanford, C., Hsu, D. J., and Telgarsky, M. (2024). Representational strengths and limitations of transformers. *Advances in Neural Information Processing Systems*, 36.
- Sarker, M. I., Losada-Gutiérrez, C., Marron-Romera, M., Fuentes-Jiménez, D., and Luengo-Sánchez, S. (2021). Semi-supervised anomaly detection in video-surveillance scenes in the wild. *Sensors*, 21(12):3993.
- Saypadith, S. and Onoye, T. (2021). An approach to detect anomaly in video using deep generative network. *IEEE Access*, 9:150903–150910.
- Steed, R. and Caliskan, A. (2021). Image representations learned with unsupervised pre-training contain human-like biases. In *Proceedings of the 2021 ACM conference on fairness, accountability, and transparency*, pages 701–713.
- Sultani, W., Chen, C., and Shah, M. (2018). Real-world anomaly detection in surveillance videos. In *Proceedings of the IEEE conference on computer vision and pattern recognition*, pages 6479–6488.
- Sun, C., Jia, Y., Song, H., and Wu, Y. (2020). Adversarial 3d convolutional auto-encoder for abnormal event detection in videos. *IEEE Transactions on Multimedia*, 23:3292–3305.
- Sun, X., Chen, J., Shen, X., and Li, H. (2022). Transformer with spatio-temporal representation for video anomaly detection. In *Joint IAPR International Workshops on Statistical Techniques in Pattern Recognition (SPR) and Structural and Syntactic Pattern Recognition (SSPR)*, pages 213–222. Springer.
- Suresha, M., Kuppa, S., and Raghukumar, D. (2020). A study on deep learning spatiotemporal models and feature extraction techniques for video understanding. *International Journal of Multimedia Information Retrieval*, 9:81–101.
- Ullah, W., Hussain, T., Ullah, F. U. M., Lee, M. Y., and Baik, S. W. (2023). Transcnn: Hybrid cnn and transformer mechanism for surveillance anomaly detection. *Engineering Applications of Artificial Intelligence*, 123:106173.
- Ullah, W., Ullah, A., Haq, I. U., Muhammad, K., Sajjad, M., and Baik, S. W. (2021a). Cnn features with bi-directional lstm for real-time anomaly detection in surveillance networks. *Multimedia tools and applications*, 80:16979–16995.
- Ullah, W., Ullah, A., Hussain, T., Khan, Z. A., and Baik, S. W. (2021b). An efficient anomaly recognition framework using an attention residual lstm in surveillance videos. *Sensors*, 21(8):2811.
- Vaswani, A., Shazeer, N., Parmar, N., Uszkoreit, J., Jones, L., Gomez, A. N., Kaiser, Ł., and Polosukhin, I. (2017). Attention is all you need. *Advances in neural information processing systems*, 30.
- Wang, G., Wang, Y., Qin, J., Zhang, D., Bao, X., and Huang, D. (2022). Video anomaly detection by solving decoupled spatio-temporal jigsaw puzzles. In *European Conference on Computer Vision*, pages 494–511. Springer.
- Wang, L., Tian, J., Zhou, S., Shi, H., and Hua, G. (2023). Memory-augmented appearance-motion network for video anomaly detection. *Pattern Recognition*, 138:109335.
- Wu, J.-C., Hsieh, H.-Y., Chen, D.-J., Fuh, C.-S., and Liu, T.-L. (2022). Self-supervised sparse representation for video anomaly detection. In *European Conference on Computer Vision*, pages 729–745. Springer.
- Yang, Z., Liu, J., and Wu, P. (2021). Bidirectional retrospective generation adversarial network for anomaly detection in videos. *IEEE Access*, 9:107842–107857.
- Yang, Z., Wu, P., Liu, J., and Liu, X. (2022). Dynamic local aggregation network with adaptive clusterer for anomaly detection. In *European Conference on Computer Vision*, pages 404–421. Springer.
- Yu, S., Zhao, Z., Fang, H., Deng, A., Su, H., Wang, D., Gan, W., Lu, C., and Wu, W. (2023). Regularity learning via explicit distribution modeling for skeletal video anomaly detection. *IEEE Transactions on Circuits and Systems for Video Technology*.
- Yu, W. and Huang, Q. (2022). A deep encoder-decoder network for anomaly detection in driving trajectory behavior under spatio-temporal context. *International Journal of Applied Earth Observation and Geoinformation*, 115:103115.
- Yuan, Y., Fang, J., and Wang, Q. (2014). Online anomaly detection in crowd scenes via structure analysis. *IEEE transactions on cybernetics*, 45(3):548–561.

- Zaheer, M. Z., Mahmood, A., Khan, M. H., Segu, M., Yu, F., and Lee, S.-I. (2022). Generative cooperative learning for unsupervised video anomaly detection. In *Proceedings of the IEEE/CVF conference on computer vision and pattern recognition*, pages 14744–14754.
- Zeng, X., Jiang, Y., Ding, W., Li, H., Hao, Y., and Qiu, Z. (2021). A hierarchical spatio-temporal graph convolutional neural network for anomaly detection in videos. *IEEE Transactions on Circuits and Systems for Video Technology*.
- Zhang, D., Huang, C., Liu, C., and Xu, Y. (2022). Weakly supervised video anomaly detection via transformer-enabled temporal relation learning. *IEEE Signal Processing Letters*, 29:1197–1201.
- Zhang, W., Wang, G., Huang, M., Wang, H., and Wen, S. (2021). Generative adversarial networks for abnormal event detection in videos based on self-attention mechanism. *IEEE Access*, 9:124847–124860.
- Zhao, C., Chang, X., Xie, T., Fujita, H., and Wu, J. (2023). Unsupervised anomaly detection based method of risk evaluation for road traffic accident. *Applied Intelligence*, 53(1):369–384.
- Zhu, S., Chen, C., and Sultani, W. (2020). Video anomaly detection for smart surveillance. In *Computer Vision: A Reference Guide*, pages 1–8. Springer.
- Zhu, Y., Bao, W., and Yu, Q. (2022). Towards open set video anomaly detection. In *European Conference on Computer Vision*, pages 395–412. Springer.